PREDICTION AND ANALYSIS OF THE LOW SPEED STALL CHARACTERISTICS OF THE BOEING 747

by

William McIntosh
John K. Wimpress

The Boeing Company
Seattle, Washington
98124 U.S.A.

SUMMARY

It is important to estimate accurately the stall speed of a modern high-speed transport since take-off and landing performance, which has a large impact on the airplane's economic success, is based on this parameter.

The pre-flight estimates for the Boeing 747 were based on wind tunnel data obtained at a Reynolds number of approximately 1 million. These test results were adjusted to full scale flight values using correlation factors developed from other Boeing transport airplanes. As an independent check, high lift data were obtained in a pressurized wind tunnel up to a Reynolds number of 7.5 million and extrapolated to the full scale value of 40 million.

Flight results show that the correlation factors were moderately successful in predicting stall speeds. However, extrapolating the pressure tunnel data to full scale Reynolds numbers predicted the flight value of maximum lift coefficient with reasonable accuracy.

The empirical approach taken to predict the 747 stall speeds does not lead to any fundamental understanding of the physics of the stall. Therefore, a further analysis was undertaken that showed that the inclusion of aeroelastic and airplane dynamics in a stall analysis can explain quite well the demonstrated flight test speeds, and in particular the gross weight effect on the stall lift coefficient.

The wind tunnel data at all Reynolds numbers predicted satisfactory handling characteristics throughout the stall that were confirmed during flight testing.

1. INTRODUCTION

Modern jet transport airplanes normally fly at speeds well separated from their low speed stalls. There is no need for them to perform extreme maneuvers at low or moderate speeds or at high altitudes that might force them near their maximum lift coefficient. Only during take-off and landing, where the lowest possible speed is desired, does the stall become a matter of concern in the design. In these two critical phases of flight, the operational speeds must be such that adequate margin exists for atmospheric turbulence and piloting tolerance and that sufficient lift is available for necessary maneuvering. The magnitudes of these margins have been established through many years of experience and are defined, with but minor variations, by the various certificating agencies throughout the world, both military and civil. Usually, the operational speeds for take-off and landing are defined in terms of the stall speed of the airplane in the same configuration.

These operational speeds in turn define the useable take-off and landing field lengths of the airplane. The useable field lengths have a large impact on the economic usefulness of the transport, so much effort is exerted in making the operational speeds as low as possible. Thus, there is a desire to make the stall speed low and also to predict it accurately early in the design stages when the initial sales guarantees are being made. The initial predictions will be made several years before the airplane flies, and even the detail predictions for the final production configuration will be made some two years before the airplane is certified.

The importance of making the stall speed prediction accurately is demonstrated by considering the case where the airplane is designed to land with a full payload in exactly the field length available at its destination. In this case, an error of only 5 percent in predicting the stall speed will result in a 38 percent loss in payload capability and an even more dramatic 55 percent loss in the potential profit available to the operator on this particular mission.

The initial estimate of the stall speed of the 747 was made early in 1966 during negotiations with Pan American World Airways, the original buyer. These predictions were steadily refined during the design development of the airplane. Development of the low speed configuration involved some 4000 hours of wind tunnel testing over a period of 3-1/2 years. Many different configurations were considered, but this paper will discuss only the final configuration selected for production and the methods used to predict and analyze the full scale performance.

The methods used to predict the full scale flight performance, starting from the wind tunnel data of the final configuration, were not particularly elegant from the standpoint of theoretical aerodynamics. They involved no detailed analysis of the boundary layer or effect of Reynolds number on the various high-lift components. The approach used was one of practical engineering, limited in scope by the usual restrictions of time, people, and money. At the time the 747 was being developed, Boeing had already built and tested a series of jet transport having sweptback wings, different engine installations, and largely varying gross weights. This experience provided a great bank of flight data that could be correlated with the corresponding wind tunnel data as a function of configuration, center of gravity position, and wing loading. These correlations served as the primary bridge between the wind tunnel data and the predicted full scale performance of the 747.

However, the 747 had a leading edge flap that was markedly different from those on other Boeing airplanes, and therefore, it was felt necessary to evaluate the effects of Reynolds number on these leading-edge flaps. High Reynolds number tests were made that extended the wind tunnel data from a Reynolds Number of approximately 1 million up to 7.5 million, based on the wing mean aerodynamic chord.

The flight test results shown in this paper are those obtained during the Federal Aviation Agency (FAA) certification of the 747. A total of 636 instrumented stalls were conducted to get stall speed data at all flap settings and gross weights and to completely evaluate the handling characteristics during the stall maneuver. A remote sensor of static pressure trailing behind the airplane was used for all air speed measurements. Accelerometers and rate and position gyros were used to establish the airplane motions, and a calibrated fuselage-mounted vane was used for measuring angle of attack.

Subsequent to the 747 flight tests an analysis was undertaken to determine if some of the anomalies inherent in the prediction versus test results correlation could be explained in a rational manner. The approach taken was to start from the same low Reynolds number wind tunnel data used in the prediction method and apply corrections for Reynolds number, Mach number, aeroelastic deflections and stall maneuver dynamics. The results from this analysis process were then compared with the flight test results.

2. DESCRIPTION OF THE 747 HIGH LIFT SYSTEM

A diagram of the 747 high lift system is shown in Figure 1. The wing has an aspect ratio of 7 and is swept back 37-1/2 degrees at the quarter chord. Both leading-edge and trailing-edge high lift devices are used. The leading-edge devices cover the entire span of the wing except for a small region next to the body. Inboard of the inboard nacelle is a flat Krueger flap with a rounded nose similar to that used on the 707. Between the nacelles, and outboard of the outboard nacelle, the Krueger flap is more sophisticated. As the flap is extended, a mechanical linkage bends the skin to form a continuous curve throughout its length. Also, the flap moves far enough forward to create a slot between it and the wing leading edge. This installation was the first time such a curved, slotted, Krueger flap had been used on a Boeing airplane.

The trailing-edge flaps extend from the body to approximately 70 percent of the span. The flap is divided into two major components separated to allow clearances for the jet efflux of the inboard engine. This space on the trailing edge is used for the inboard high-speed aileron. The trailing-edge system is triple-slotted, similar to that used on the 727 and 737, but tailored to the long-range mission of the 747. For take-off, the flap setting, as measured by the angle of the mid-segment, varies between 10 and 20 degrees, depending on take-off weight. The motion includes a great deal of Fowler action before much angular deflection occurs. For landing, the flap is extended to its full 33 degree deflection.* The various settings were selected after consideration of both the lift and drag, and the corresponding effects on field length performance, post-take-off climb, and go-around after a refused landing.

During the design of the 747 flap system, it was recognized that flap system design would be subject to some aeroelastic deflections, particularly on the leading edge devices which are basically flexible fiberglass panels. The flaps were designed so that under load they conformed to the angles and shapes defined during the wind tunnel development of the 747.

3. THE BASIC WIND TUNNEL DATA

The basic low-speed wind tunnel data were obtained in the University of Washington Aeronautical Laboratory wind tunnel, which has an 8 foot by 12 foot closed test section vented to the atmosphere. The model, shown in Figure 2, was an .04 scale replica of the 747 having a wing span of approximately 8 feet. This model duplicated carefully all the flap supports and fairings as well as all the contours, gaps, and slots that exist on the production airplane.

The wing was also twisted to simulate the aeroelastic deflections encountered during flight. Particular care was taken, since our experience has shown that many of the discrepancies between wind tunnel and flight, often blamed on scale effects, are in fact caused by an inadequate representation of the details of the flight configuration by the wind tunnel model. The data for representing the airplane flying near to the ground were obtained using a fixed ground plane.

An example of the data obtained from this model is shown in Figure 3. Normal wall and blockage corrections have been applied. Data is shown for a landing flap configuration of 33 degrees and typical take-off positions of 10 degrees and 20 degrees.

4. THE STALL MANEUVER

Several full scale parameters must be estimated from this lift and pitching moment data as indicated in Figure 4, which shows the flight records obtained during a typical flight test stall. The principle item to be estimated is the Federal Aviation Regulation (FAR) stall speed. This speed is defined as the minimum speed obtained during a full stall that is approached at the rate of 1 knot per second. This minimum speed occurs during a dynamic maneuver, and the airplane usually will be somewhere between .80 and .90 g's at the time this minimum speed is reached. This FAR stall speed is used by the FAA as one consideration in determining take-off and landing speeds for airplanes certified within the United States. The corresponding FAR $C_{L_{Stall}}$ is defined at $C_{L_{Stall}} = \frac{W}{1/2\rho V^2_{Stall} S} = \frac{W}{qS}$ without considering the reduced load factor existing at the time V_{Stall} occurs. Another stall speed is the 1 g stall speed, which is defined as that speed which occurs just as the normal acceleration breaks to a reduced value. This speed also is measured during a dynamic maneuver and may not occur at exactly 1 g normal acceleration. This 1 g stall speed is used as the basis for setting the take-off and landing speeds by the U.S. Air Force. The corresponding C_L historically has been used as $C_{L_{max}}$ in the structural analysis of the airplane. Also to be estimated, is the true $C_{L_{max}}$ achieved during the stall maneuver, where C_L is defined as $\frac{nW}{qS}$. This maximum lift coefficient usually occurs at a speed below the 1 g stall speed and is the flight $C_{L_{max}}$ most nearly corresponding to the one measured in a wind tunnel test.

5. CORRELATION CURVES AND FLIGHT TEST RESULTS

5.1 FAR $C_{L_{Stall}}$ and $C_{L_{max}}$

Figure 5 summarizes the high-lift flight and wind tunnel data from a series of Boeing airplanes by showing the ratio of the FAR $C_{L_{Stall}}$ to the wind tunnel $C_{L_{max}}$. The data shows appreciable scatter between airplanes, and the solid line was chosen as the value of the parameter to be used in estimating the 747 performance. The 747 flight test results generally lie somewhat below this estimated value. The data points shown in the upper part of the chart are for the airplanes at the maximum weights tested. The lower plot presents the trend of the stall speeds as a function of airplane wing loading, and shows that increasing gross weight decreases slightly the stall lift coefficient. This wing loading effect has been consistent throughout the history of Boeing airplanes. The values of wind tunnel $C_{L_{max}}$ used to develop these plots differs slightly from those shown in Figure 3. The reason is that there were no blockage corrections used in reducing the 747 wind tunnel data shown here. This was done in order to compare with the previous tests of the Boeing family, made before blockage corrections were a normal part of the wind tunnel data reduction procedure.

* Called "position 30" in the flight handbook

A similar summary of the 1 g $C_{L_{Stall}}$ is shown in Figure 6. Again, there is appreciable scatter in the data, and the solid line represents the value used in making the 747 pre-flight estimate. The 747 flight test results gave 1 g $C_{L_{Stall}}$'s as much as 8 percent below the original estimate. This fact is particularly surprising since a test installation of the 747-type leading-edge flap on a 707 gave a correlation factor well above the other airplanes. The 1 g $C_{L_{Stall}}$ showed the same trend with wing loading as was indicated for the FAR $C_{L_{Stall}}$.

At the time these estimates were being made, it was recognized that the 747 had a leading-edge device that might render past wind-tunnel-to-flight-test correlations inaccurate. Past Boeing airplanes had a leading-edge device, either Krueger flap or slat, that was relatively sharp, creating high pressure peaks and rapid pressure recoveries which would make the flow sensitive to Reynolds number effects. The 747, on the other hand, had a leading-edge device that was carefully designed using aerodynamic theory to produce a smooth pressure distribution having no severe gradients at high angles of attack. With the gradient selected to give no separations at low Reynolds number, no appreciable increase in lift should be expected as Reynolds number is increased.

In order to evaluate these considerations, a wind tunnel test was made in the 12 foot pressure tunnel at the Ames Aeronautical Laboratory of the NASA where the Reynolds number could be varied from approximately 1.2 million up to 7.5 million. These data, shown in Figure 7, are in good agreement at low Reynolds number with the data obtained in the University of Washington wind tunnel when corrected to the forward center of gravity position used in this figure. The increase in $C_{L_{max}}$ with Reynolds number was relatively modest, and the data showed enough linearity to allow extrapolation to the full scale Reynolds number of 30 to 40 million. The flight test data shown are the maximum C_L's achieved in the stall ($C_{L_{max}} = \frac{nW}{qS}$) and indicate an agreement within 2 percent or less of the extrapolated wind tunnel values.

5.2 C_L's for Minimum Un-Stick Speed

FAA certified lift-off speeds are related to the minimum speed that the airplane can demonstrate a complete take-off, called V_{MU}. The lift coefficient for this condition can be limited by either $C_{L_{max}}$ or by the angle of attack existing when the aft body contacts the ground. Therefore, it is necessary to estimate both the lift curve shape and the $C_{L_{max}}$ in ground effect. The basic data for making this estimate were obtained in the wind tunnel using a fixed ground plane modified to allow unusually high pitch attitudes, as shown in Figure 8. The lift curve so established was checked at high Reynolds number and found to be essentially unchanged. Since angle of attack is such an important parameter under these conditions, the model used for this test had the wing twisted to represent the aeroelastic distortion of the actual airplane during heavy weight, flaps down, flight. These wind tunnel data were then corrected by correlation factors obtained on previous Boeing aircraft similar to those shown for the free-air conditions. Resultant pre-flight estimates and subsequent flight data are shown in Figure 9. The data shows a scatter of ± 5 percent, typical of flight test information taken during the take-off phase. However, it does straddle very well the pre-flight estimate. A picture of this rather dramatic flight testing for $C_{L_{max}}$ in ground effect is shown in Figure 10.

5.3. Pitching Moments

The static longitudinal pitching moments play an important role in determining the handling characteristics of the airplane during the stall maneuver. The influence of aeroelastic deflections and local separations on a swept wing can have large effects on wing pitching moments.

Separations on the wing, body, and nacelles can influence the tail contribution to stability. Since these separations can be sensitive to Reynolds number effects, it is difficult to predict the airplane's full-scale behavior if the wind tunnel data indicate a situation that is marginal in any way. At Boeing, our philosophy has been for many years to design for good pitching moment characteristics under low Reynolds number conditions to assure good characteristics in flight. A small pitch-up in the stall is permissible and tends to hold the airplane to a slightly lower speed before it pitches down out of the stall. This permissible pitch-up must cause only a limited excursion in angle of attack, say 4 to 6 degrees, involve essentially no increase in C_L once the pitch-up begins, and must be followed by strong pitch-down to assure a good clean break away from the stall.

The wind tunnel pitching moment data at both low and high Reynolds number and the corresponding flight data are compared in Figure 11. There is practically no change in wind tunnel pitching moment data with Reynolds number probably a result of the cambered leading-edge flap. The flight data show slightly superior stability at stall entry than the wind tunnel data indicate. They also show that the wind tunnel predicted quite accurately the flight values for the angle of incipient pitch-up and the angle of recovery. These pitching moment characteristics produced an airplane extremely easy to fly thoroughout the stall maneuver.

6. STALL MANEUVER ANALYSIS

6.1 Stall Parameters

While the stall speed prediction method used for the 747 was moderately successful such a procedure does not lead to any fundamental understanding of the physics of the stall. Consequently an analysis was undertaken to get some appreciation of the factors involved in the stall. The parameters that have been considered in the 747 stall analysis are:

1. Reynolds number
2. Mach number
3. Aeroelastic effects
4. Pitchup characteristic
5. Pitch inertia
6. Stall entry rate
7. Stall technique

The influence of the last four items of the list can only be assessed in a dynamic stall simulation. A three degree of freedom digital simulation was undertaken to determine these effects.

6.2 Reynolds and Mach Number Effects

The Reynolds number effects were assessed by using the low Reynolds number data obtained at the University of Washington wind tunnel and extrapolating to full scale using the higher Reynolds number data obtained in the 12 foot pressure tunnel at the Ames Aeronautical Laboratory of the NASA. This extrapolation was augmented by some two dimensional high Reynolds number data obtained on the 747 flap system at the 5 x 5 foot variable density tunnel of the National Aeronautical Establishment (NAE) in Ottowa, Canada. This two dimensional data was taken over a Reynolds number range of 1.25×10^6 to 13.0×10^6. These data confirm the trend shown in Figure 7 which indicates quite a modest Reynolds number effect on $C_{L_{max}}$. This mild Reynolds number sensitivity for the 747 is due to the careful design which produced a smooth pressure distribution on the flaps having no severe gradients at high angles of attack. Reynolds number effects on earlier flap systems with severe gradients can be much larger as shown on Figure 12.

The basic low Reynolds number data at the University of Washington tunnel were obtained at a relatively low Mach number of M = .16. During a flight test stall the Mach number may be as high as M = .30. Due to the very high negative pressure coefficients involved on the flaps at high lift this discrepancy in Mach number could be quite serious. Therefore as a part of the test program at the NAE variable density tunnel in Canada the influence of Mach number on $C_{L_{max}}$ was also investigated. It was found that flap systems which did not take care to protect against severe pressure peaks and gradients at high angles of attack can have rather severe Mach number effects as shown on Figure 13. Because of the flap design philosophy,the influence of Mach number on the 747 $C_{L_{max}}$ is very mild.

6.3 Effect of Aeroelasticity

The influence of aeroelasticity on the stall was included by correcting the aerodynamic coefficients for aeroelastic deflections. The basic linear unstalled portion of the aerodynamic coefficients were corrected using terms derived from structural programs which use linear aerodynamics to supply the airloads.

The most difficult parameters to obtain are the aeroelastic effects near the stall. The basic 747 wind tunnel data was obtained with a wing which incorporated the aeroelastic twist for a critical flight loading case, namely the condition for a heavy weight airplane but with only partial wing fuel capacity. This condition corresponds approximately to the heavy weight stall conditions. To see the effect of the weight and fuel loading on the aeroelastic deflections consider the following cases:

	WEIGHT LBS	WING FUEL LBS	UNRELIEVED WEIGHT LBS
1.	335,000	0	335,000
2.	440,000	50,000	390,000
3.	699,000	150,000	549,000

Case 1 represents the minimum operating weight while case 2 is approximately the light weight stall conditions encountered in the 747 flight test. Case 3 is about the weight and fuel conditions encountered in the heavy weight flight test stalls. The difference in the weight deflecting the wing is quite apparent. The aeroelastic deflection associated with these loads cause a difference in span loading which on the 747 and several other Boeing airplanes causes a reduction in $C_{L_{max}}$ with increasing weight on the wing. This $C_{L_{max}}$ variation with loading should be determined by testing wind tunnel wings which have the twists and deflections associated with these loadings. Data exactly of this form are not available, however the trends do exist in the wind tunnel testing of the 747. Evidence of the aeroelastic effects are apparent in the 747 flight test data. By looking at the actual $C_{L_{max}}$ values achieved in the stall tests, a difference in maximum lift capability is apparent as shown on Figure 14. Note that the $C_{L_{max}}$ is not a function of the stall entry rate. The difference in $C_{L_{max}}$ cannot be explained in terms of Reynolds number or Mach number effects. These aeroelastic effects at the stall are part of a very complex system which is sensitive to a large number of variables and cannot be attacked except through wind tunnel testing of the range of variables involved.

To determine the total aeroelastic influence at least three cases must be evaluated, the rigid jig position wing, and at least two other deflected wings corresponding to the heavily and lightly loaded cases. The procedure used on the 747 analysis can only evaluate the increment between light and heavy loading with the total aeroelastic effect starting from the jig wing still unidentified.

6.4 Effect of Stall Dynamics

The influence of stall dynamics on stall speed was investigated using a three degree of freedom simulation which included the effects of variations in Reynolds number, Mach number and aeroelastic deflection during the stall maneuver. The simulation equations of motion are defined in Figure 15.

The FAR stall speed is specified at a stall entry rate of 1 knot per second. This entry rate is defined as follows:

$$\text{FAR entry rate} = \frac{V_{min} - 1.1V_{min}}{T_{V_{min}} - T_{1.1V_{min}}} = \frac{\Delta V}{\Delta t}$$

The flight test procedure is to perform several stalls using a consistent technique with entry rate as a variable and to plot stall speed versus entry rate to determine the FAR stall speed. The effects of stall technique, pitch inertia and pitchup were evaluated using the dynamic simulation and the FAR stall speed definition.

Using the definition of FAR stall speed it is apparent that any number of curves will pass through the points defined by V_{min} and 1.1 V_{min} and it is for this reason that stall technique is important. Two of the many possible curves are shown on Figure 16. The "slow" stall is characterized by a fairly uniform deceleration into the stall that is obtained by a gradual elevator application to a prescribed angle of attack at which the elevator is held fixed. The fast stall is characterized by a slower initial entry rate followed by a higher final entry rate. This type of stall is obtained by a slightly slower initial elevator application to some angle of attack at which full elevator is applied and held through the stall.

Two types of elevator application were devised for evaluation of the stall technique and were programmed for the simulation in order to systematically study the effect of stall entry rate and technique. A series of stall computations were then performed on the simulator to investigate the influence of gross weight, pitch up, pitch inertia and aeroelasticity on FAR stall speed. One of the simulations included the elevator input from a flight test stall to determine if the simulation was adequate. The comparison shown on Figure 17 indicates that the stall calculation simulates the flight test quite well.

6.5 Stall Simulation Results

Typical speed time histories from the simulation are shown on Figure 18 for the two types of stall entry technique with an elastic airplane. The minimum speeds and corresponding lift coefficients have been extracted and are shown plotted against stall entry rate on Figure 19. It is apparent from these data that the stall speeds are quite sensitive to both the entry rate and stall technique, but since the FAR stall is at a specified entry rate only the speed and lift coefficient at this rate are used. Similar data was obtained at lighter weights and the effects of gross weight and stall technique are shown on Figure 20. Also shown on Figure 20 are the 747 flight test results which are in reasonable agreement with the simulator generated levels.

The indicated gross weight effect on the stall lift coefficient includes the aeroelastic effects on $C_{L_{max}}$ previously shown. In order to separate the aeroelastic influence from the dynamics of the stall the light weight simulation was repeated but without the aeroelastic lift effect. The results shown on Figure 21 indicate that virtually all of the gross weight effect on the stall is due to the change in lift attributed to aeroelastic deflections.

The variation of Reynolds number, Mach number and their effects on the $C_{L_{max}}$ during the stall are shown on Figure 22. It can be seen that while there is an effect of these parameters on the $C_{L_{max}}$ neither Reynolds number nor Mach number variations are dominant factors within the stall and if the aeroelastic effect is removed both configurations achieve approximately the same lift levels.

For a given gross weight and center of gravity a considerable range of pitch inertias may be obtained. To examine the effect of this parameter on the stall the pitch inertia was changed ± 25% from the nominal value. The results indicate that the pitch inertia variations investigated have negligible effects on the FAR stall speeds. The data does indicate however that slightly faster elevator inputs are required to achieve the 1 knot per second entry rate and an effect could be found if the elevator becomes limiting.

As shown previously the pitchup at the stall is difficult to predict and some variation in the pitchup should be anticipated.

To examine the sensitivity of the FAR stall speed to the amount of pitchup, a series of simulations were performed with the pitching moments shown on Figure 23. The resulting FAR stall lift coefficients are shown on Figure 24. Over the range of pitching moments investigated, increasing the amount of pitchup has a negligible effect on the stall speeds while decreasing the amount of pitchup results in a rather serious loss in stall lift coefficient. The conclusions could be expanded into a more general statement that pitchup characteristics are not a dominant factor in the FAR stall speed determination unless the elevator capability is insufficient to develop the final stall entry rate. However, the stall characteristics at the aft center of gravity may limit the allowable pitch up and a strong pitch down after the initial pitch up must exist to assure a good clean break away from the stall.

The same simulations used to examine the FAR stall speeds were analysed to evaluate the 1 g stall speed correlation. The analyzed data presented on Figure 25 show again quite good correlation with the flight test data with the aeroelastic contribution accounting for the gross weight sensitivity. The 1 g stall speeds show a sensitivity to stall entry rate similar to the FAR stall speeds, and comparing the $C_{L_{1g}}$ values with the previously shown $C_{L_{max}}$ values it becomes apparent that the 1 g stall speeds are not obtained at unit load factor. The 1 g stall speeds are the result of the dynamics of the stall maneuver just as the FAR speeds are but at a load factor closer to unity.

A summary build up of the predicted FAR stall lift levels from low Reynolds number wind tunnel maximum lift data is shown on Figure 26. The predicted levels compare quite favorably with the values obtained during the certification flight tests. The key item is to start with a carefully designed low Reynolds number wind tunnel model twisted to a specified loading. The increments shown on Figure 26 indicate that for the 747 airplane the major influences in the buildup are the aeroelastic effect and the effect of the dynamics of the stall maneuver.

7. CLOSING REMARKS

The methods used to estimate the stall characteristics of the 747, based on the previous experience of Boeing transport airplanes, predicted the FAR stall lift coefficients within about 5 percent. This is well within the confidence band expected during the preliminary design phase of an airplane, but as shown in the introduction this is not adequate during the development and guarantee phase. A subsequent analysis considering the effects of Mach and Reynolds numbers, pitch inertia, pitchup characteristic stall technique, aeroelastics and stall dynamics has led to a better understanding and a more accurate prediction procedure for the future. The analysis has also pointed out some gaps in the data required to obtain a rational stall lift prediction.

One must conclude that the prediction of the stall lift coefficient remains a difficult engineering problem. Based on the results of the analysis of the 747 airplane much progress can be made to better understanding the physics of the stall maneuver. However there are still parts of the analysis in the area of aeroelastic effects and understanding the aerodynamics of stalled flows that should be examined in further detail to arrive at a more scientific stall prediction technique. The data required for this more scientific approach will in general not be available during the preliminary design phases of the development of an airplane and therefore the empirical procedure used for the 747 tempered with engineering judgement will still serve as a useful and reasonably accurate method for prediction.

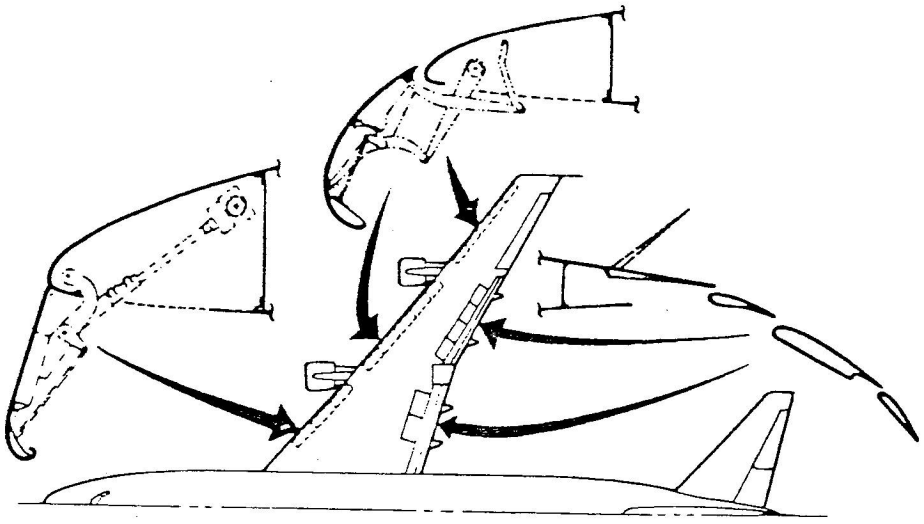

FIGURE 1: 747 HIGH LIFT SYSTEM

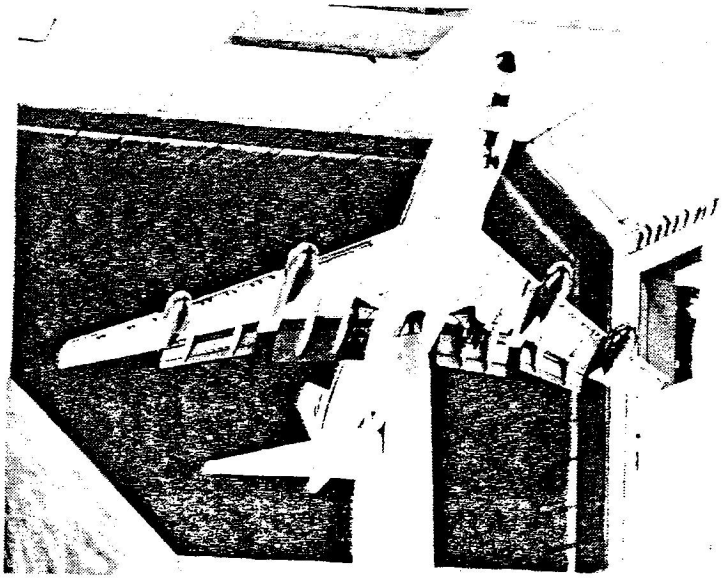

FIGURE 2: 747 HIGH LIFT WIND TUNNEL MODEL

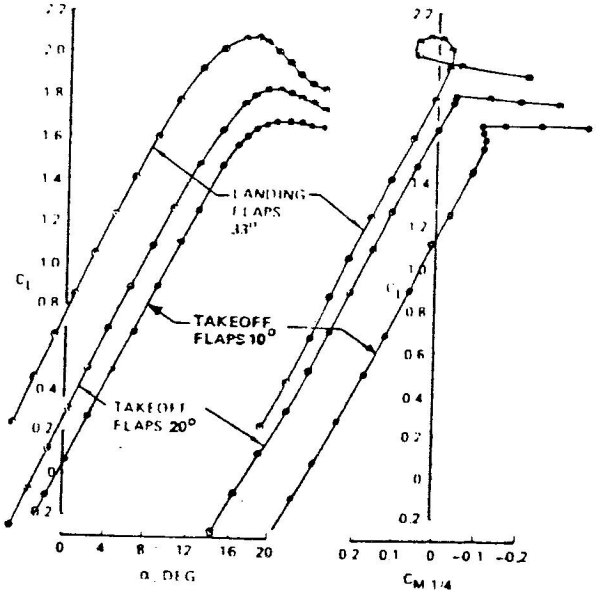

FIGURE 3: HIGH LIFT WIND TUNNEL DATA (LOW REYNOLDS NUMBER)

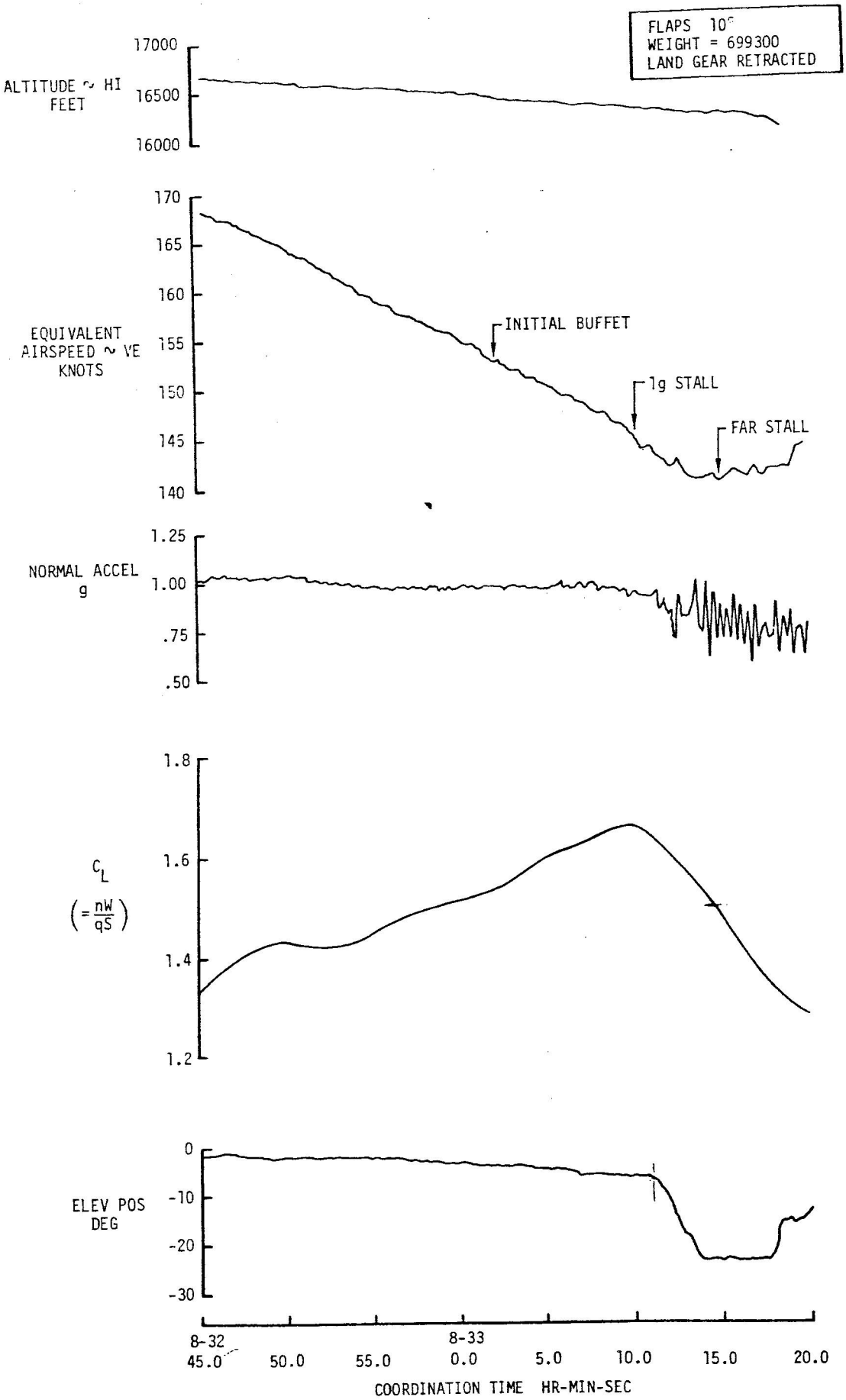

FIGURE 4: FLIGHT RECORD OF A STALL MANEUVER

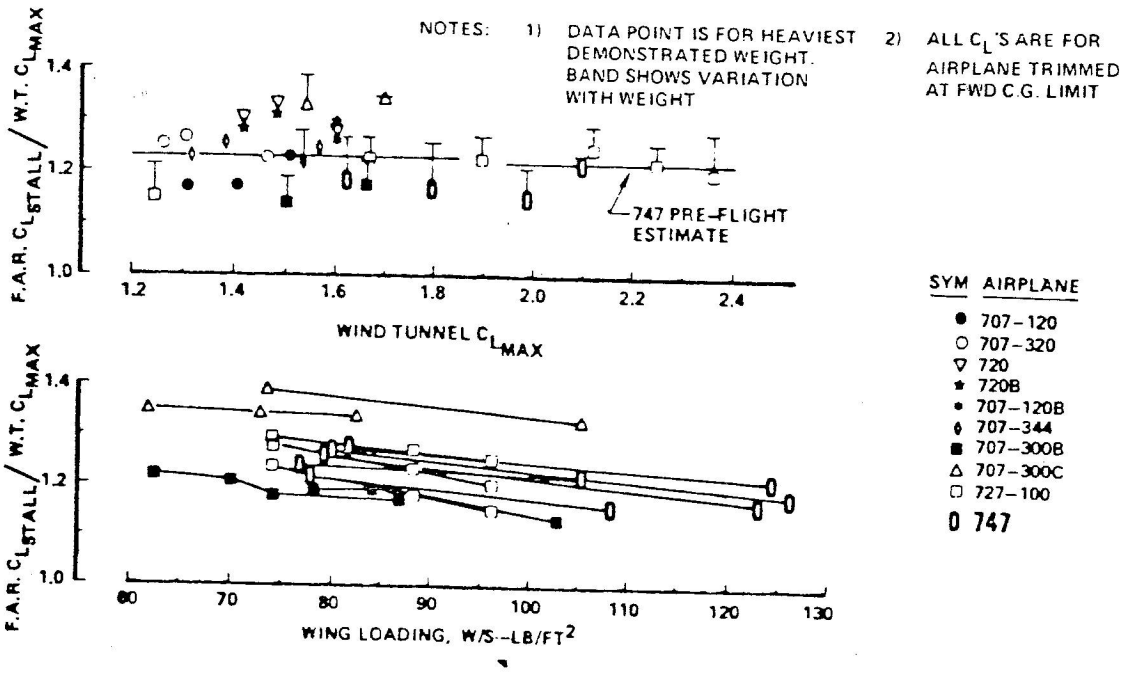

FIGURE 5: COMPARISON OF FLIGHT FAR $C_{L_{STALL}}$ AND WIND TUNNEL $C_{L_{MAX}}$

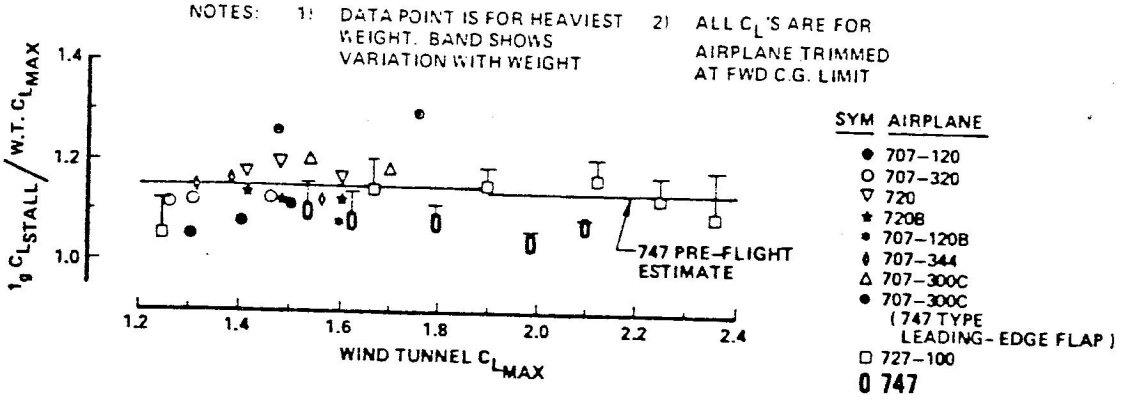

FIGURE 6: COMPARISON OF FLIGHT $1gC_{L_{STALL}}$ AND WIND TUNNEL $C_{L_{MAX}}$

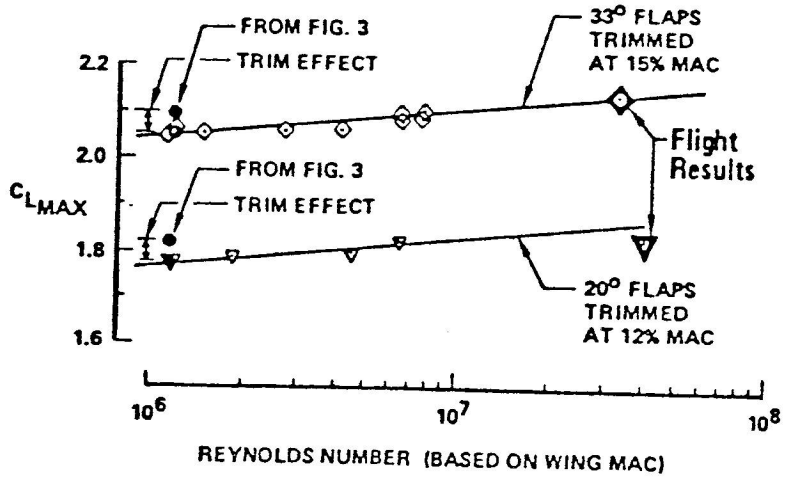

FIGURE 7: HIGH REYNOLDS NUMBER DATA

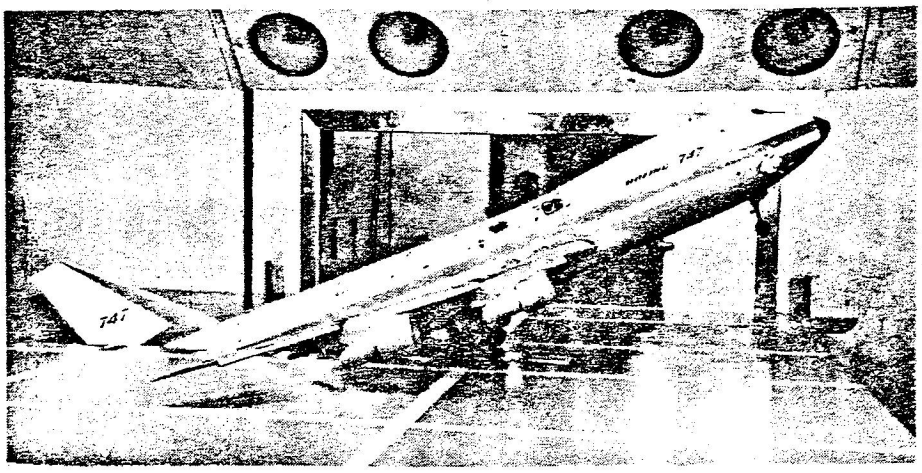

FIGURE 8: TEST FOR $C_{L_{MAX}}$ IN GROUND EFFECT

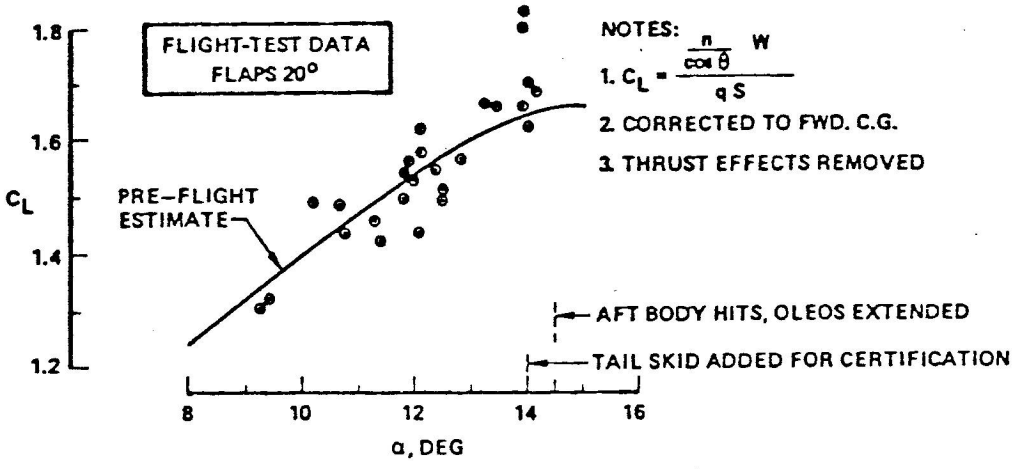

FIGURE 9: LIFT CURVE IN GROUND EFFECT

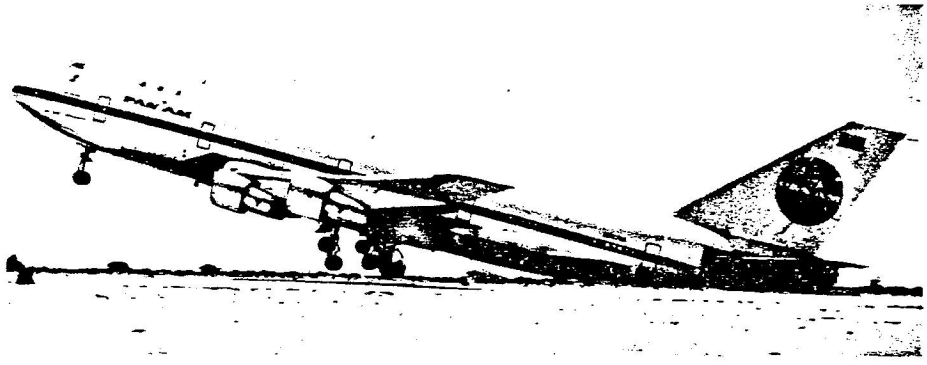

FIGURE 10: V_{MU} FLIGHT TEST

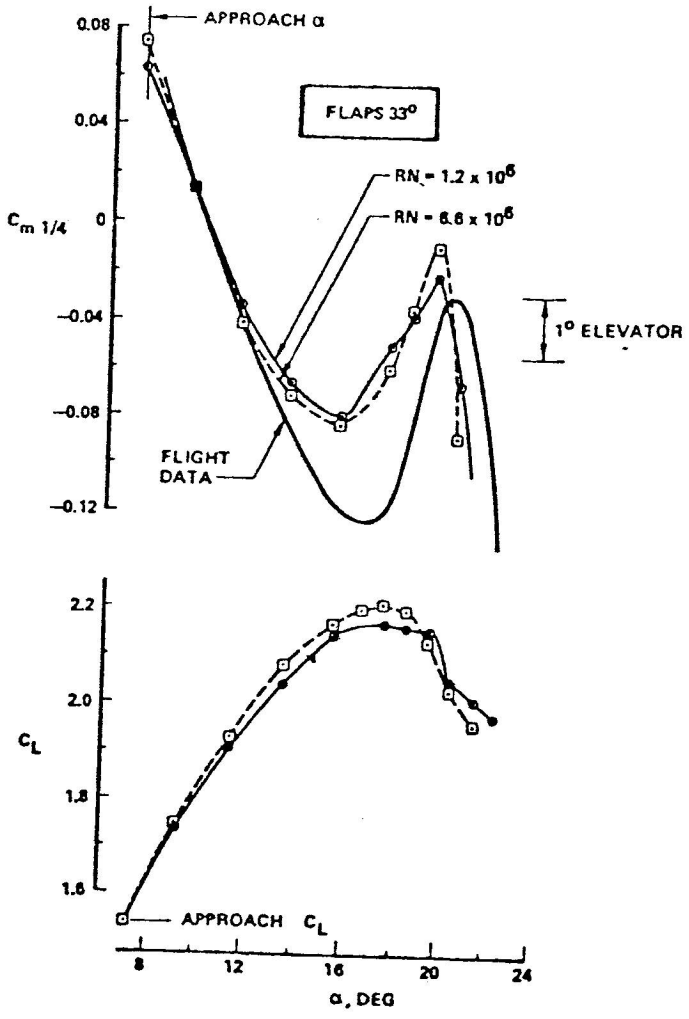

FIGURE 11: PITCHING MOMENTS IN THE STALL

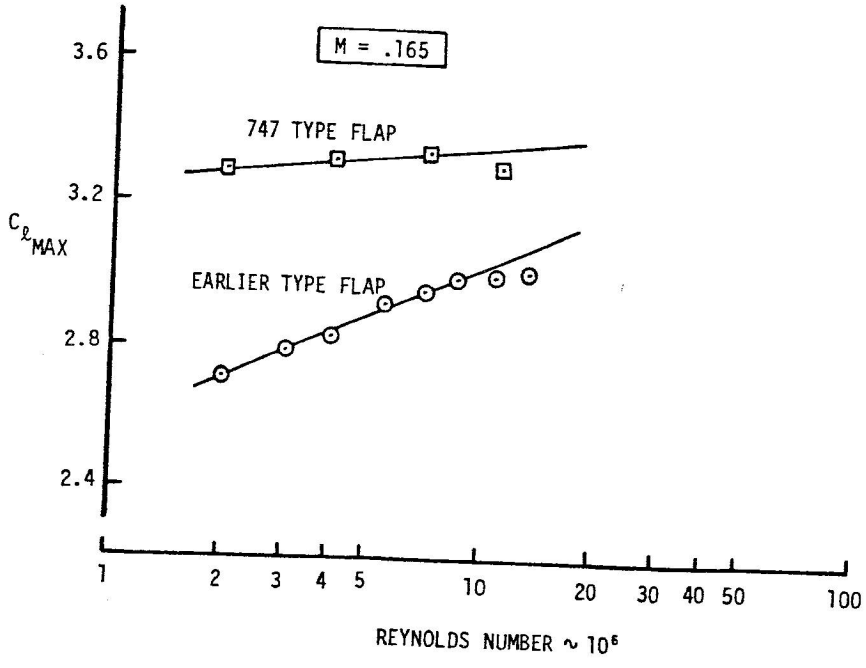

FIGURE 12: EFFECT OF FLAP TYPE AND REYNOLDS NUMBER ON TWO DIMENSIONAL MAXIMUM LIFT

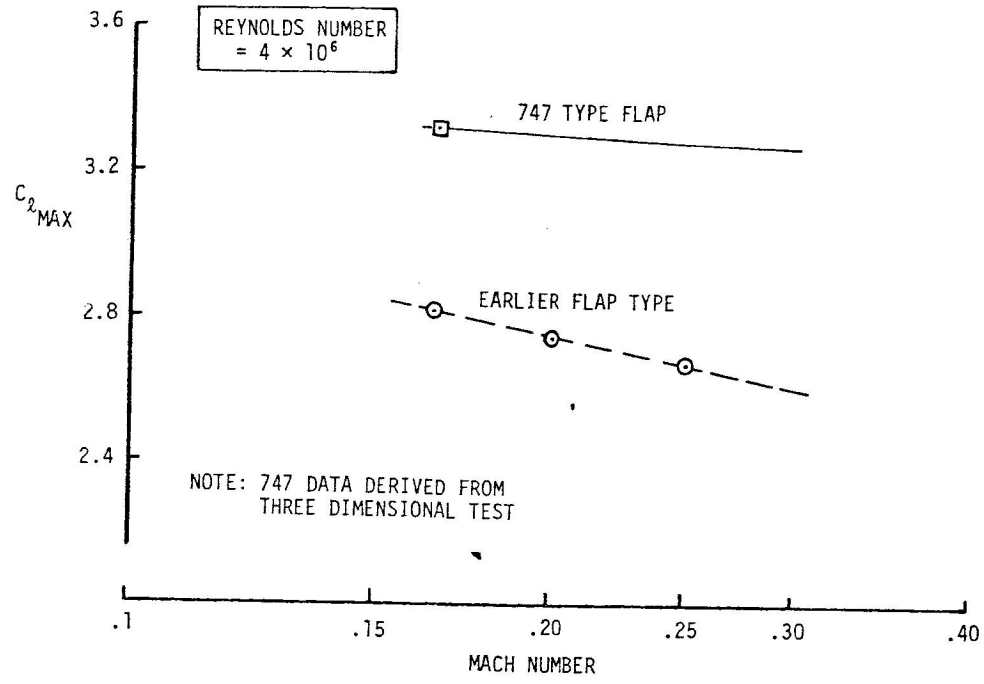

FIGURE 13: EFFECT OF FLAP TYPE AND MACH NUMBER ON TWO DIMENSIONAL MAXIMUM LIFT

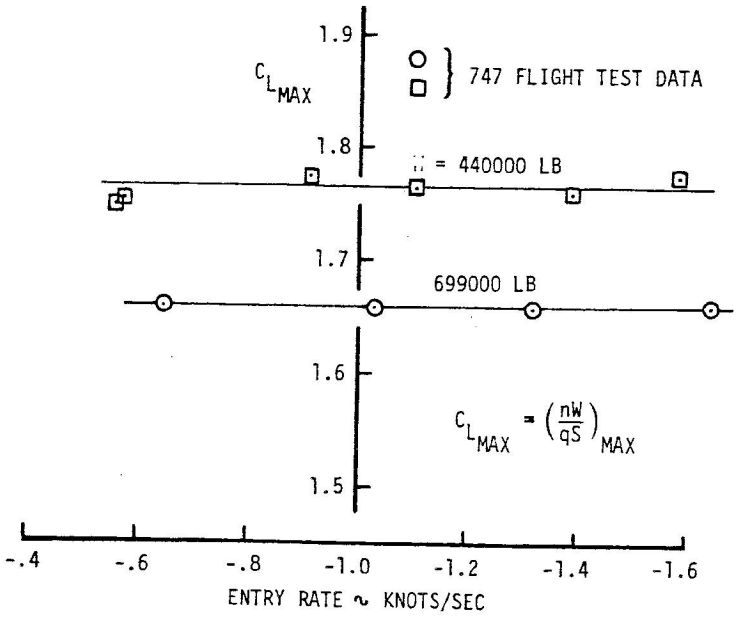

FIGURE 14: EFFECT OF GROSS WEIGHT AND ENTRY RATE ON $C_{L_{MAX}}$ ACHIEVED IN STALL

LIFT:

$$L - \frac{W}{g} V \dot{\gamma} - W \cos \gamma + T \sin (\alpha_B + i_T) = 0$$

DRAG:

$$T \cos (\alpha_B + i_T) - D - W \sin \gamma - \frac{W}{g} \dot{V} = 0$$

PITCHING MOMENT:

$$M_{ACG} + TZ_T - I_{yy} \ddot{\theta} = 0$$

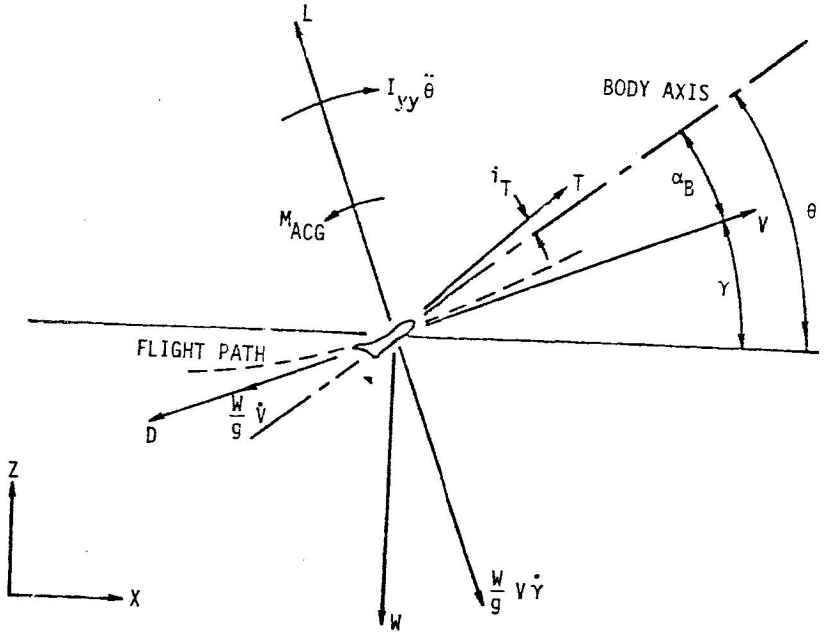

FIGURE 15: DEFINITION OF TERMS IN EQUATIONS OF MOTION

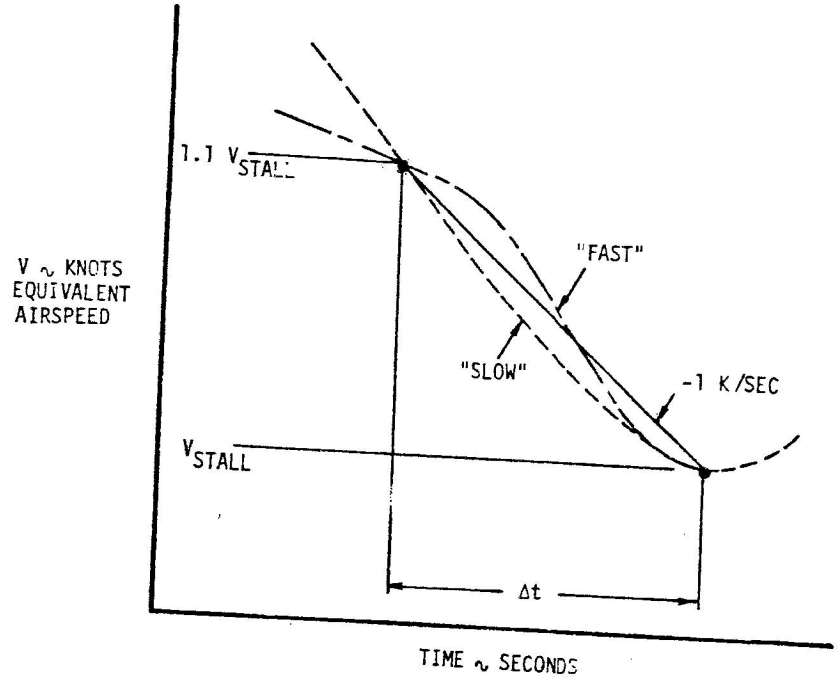

FIGURE 16: TWO TYPES OF STALL ENTRY RATE USED FOR STALL DYNAMICS STUDY

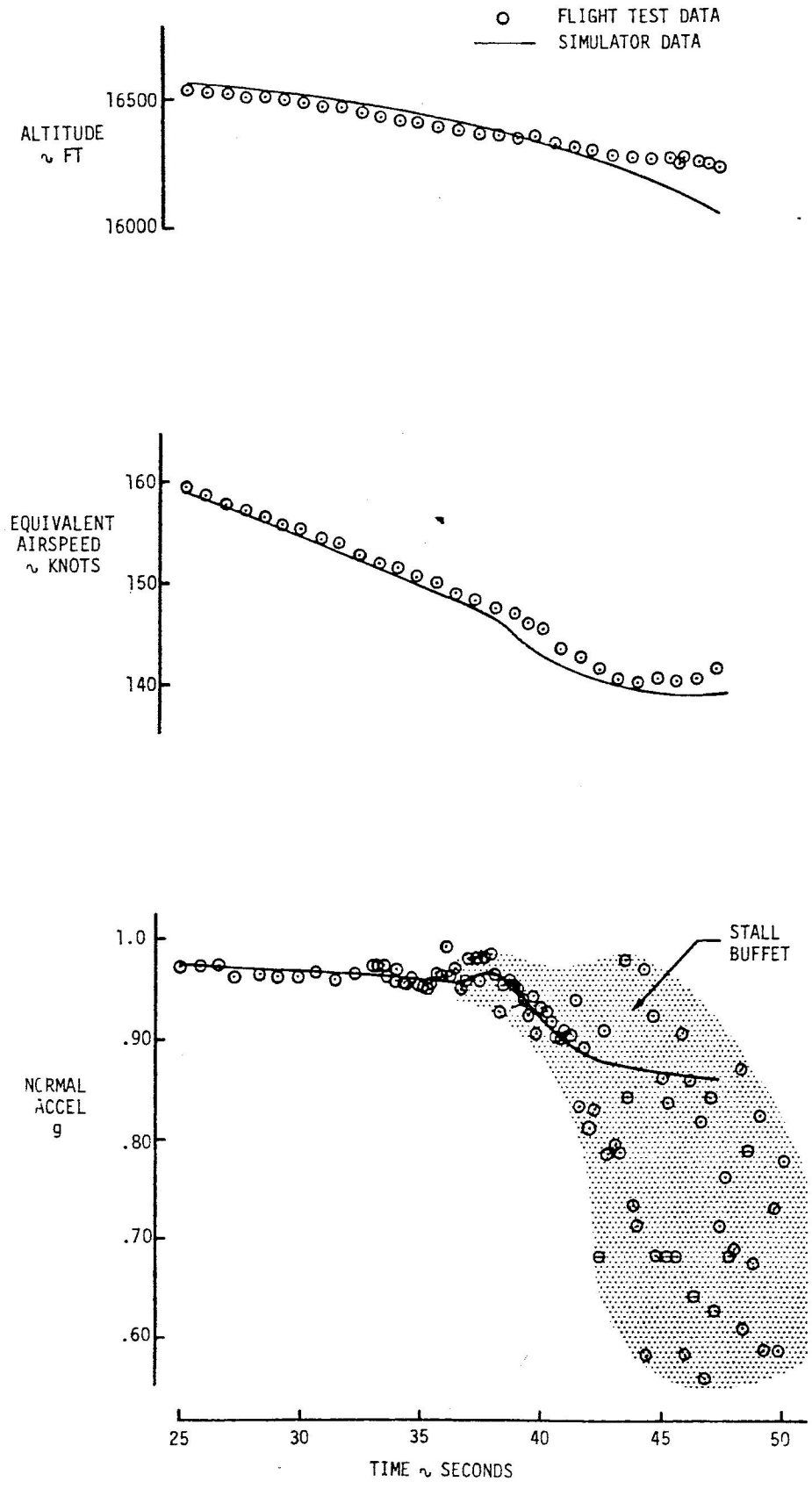

FIGURE 17: COMPARISON OF SIMULATION AND FLIGHT TEST RESULTS

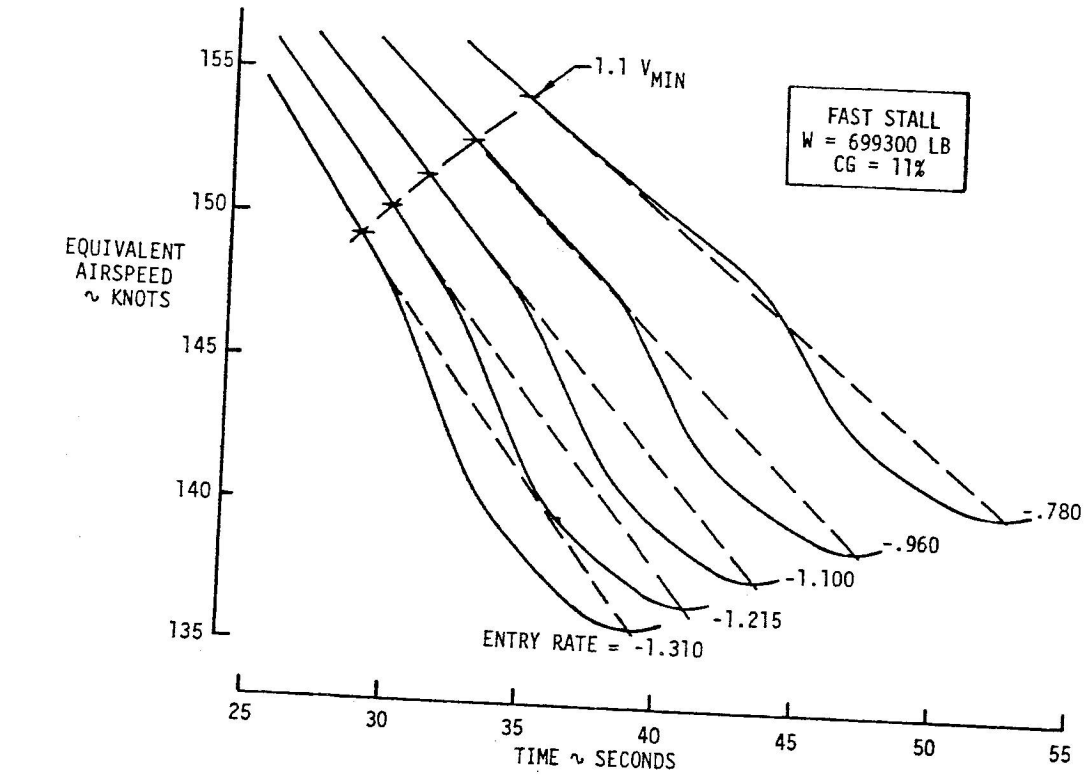

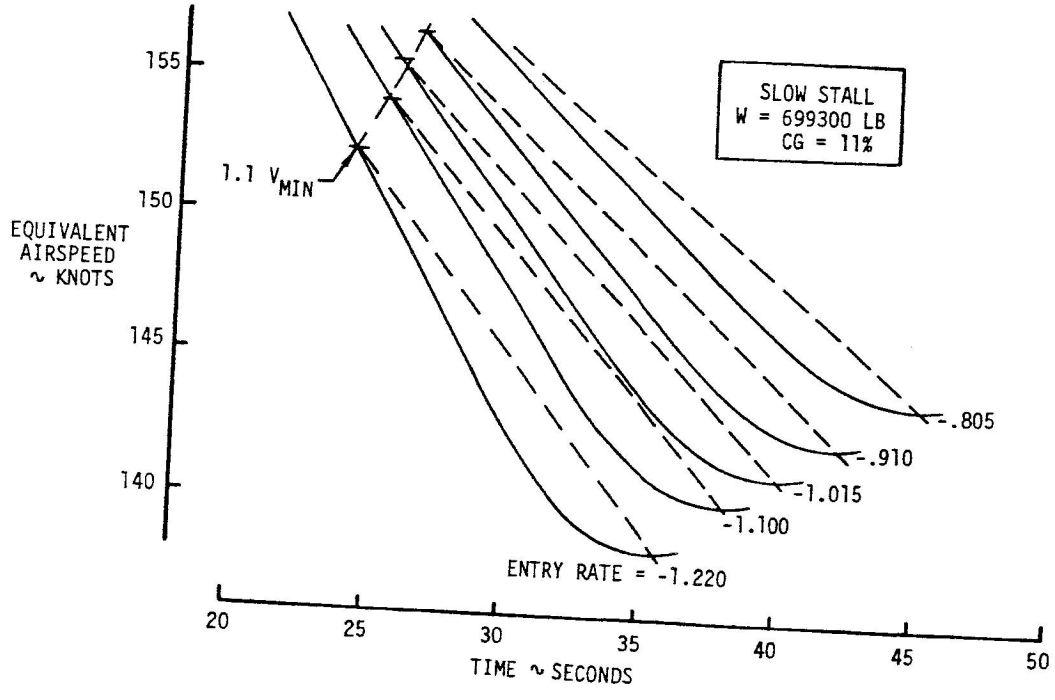

FIGURE 18: TYPICAL VELOCITY TIME HISTORIES FOR TWO TYPES OF STALL TECHNIQUE

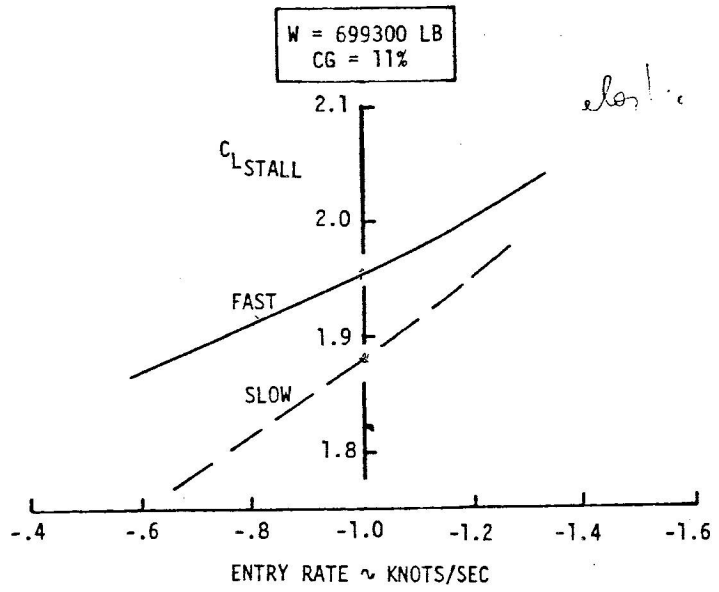

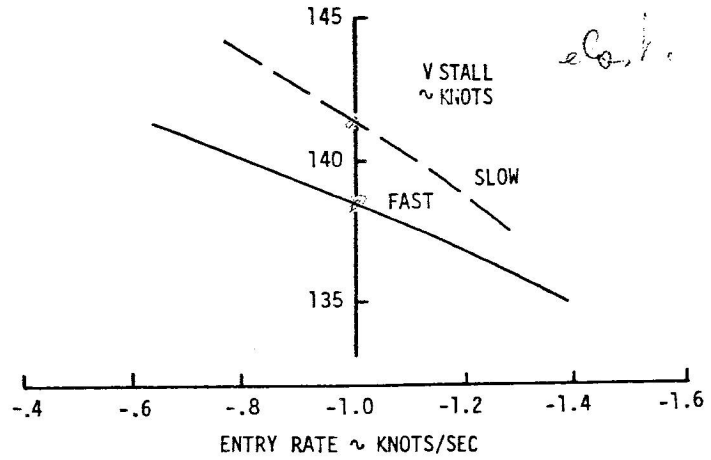

FIGURE 19: EFFECT OF STALL TECHNIQUE AND ENTRY RATE ON STALL SPEED AND LIFT COEFFICIENT

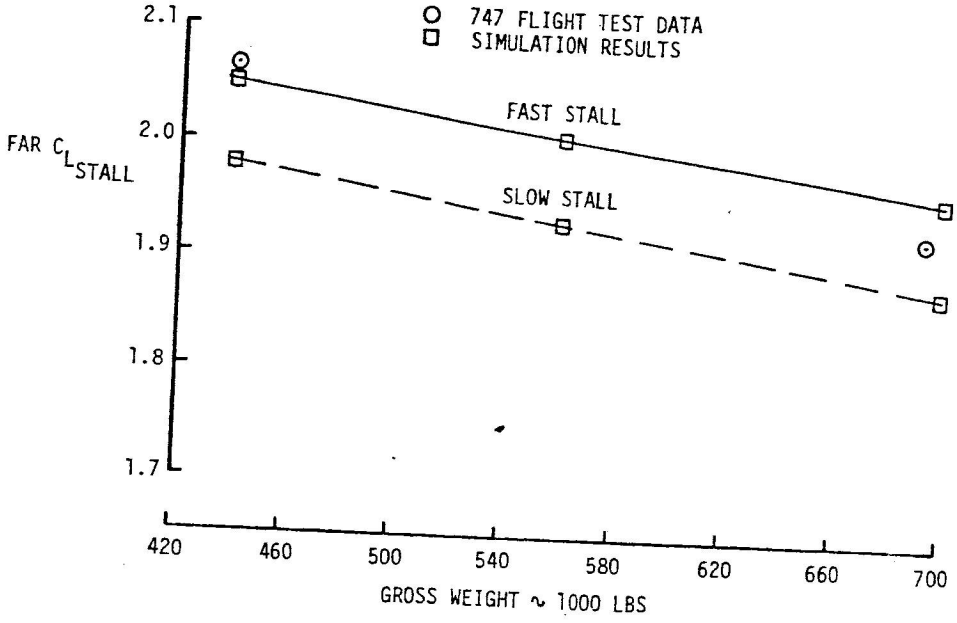

FIGURE 20: EFFECT OF STALL TECHNIQUE AND GROSS WEIGHT ON STALL LIFT COEFFICIENT

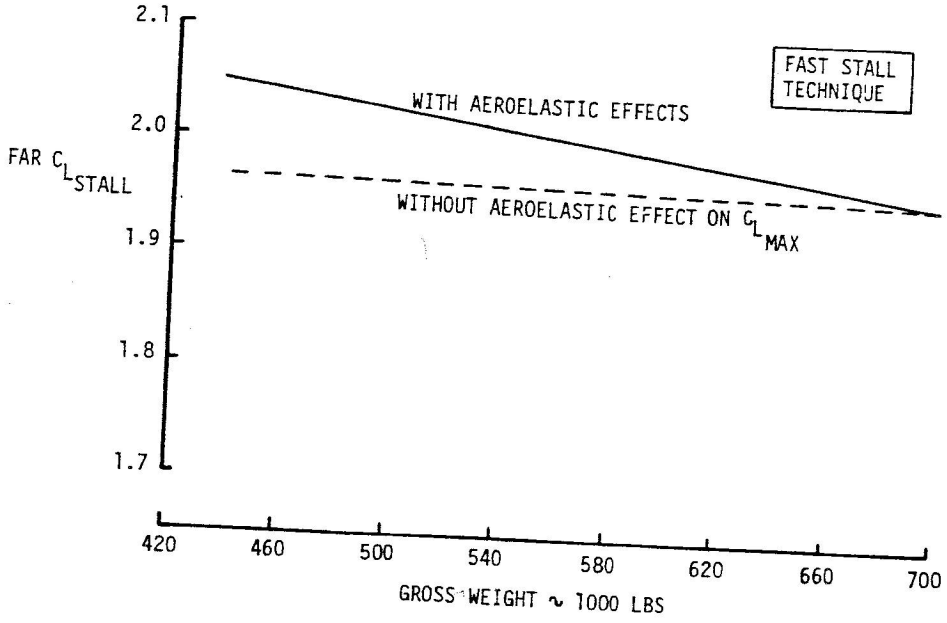

FIGURE 21: EFFECT OF AEROELASTIC LIFT INCREMENT ON STALL LIFT COEFFICIENT

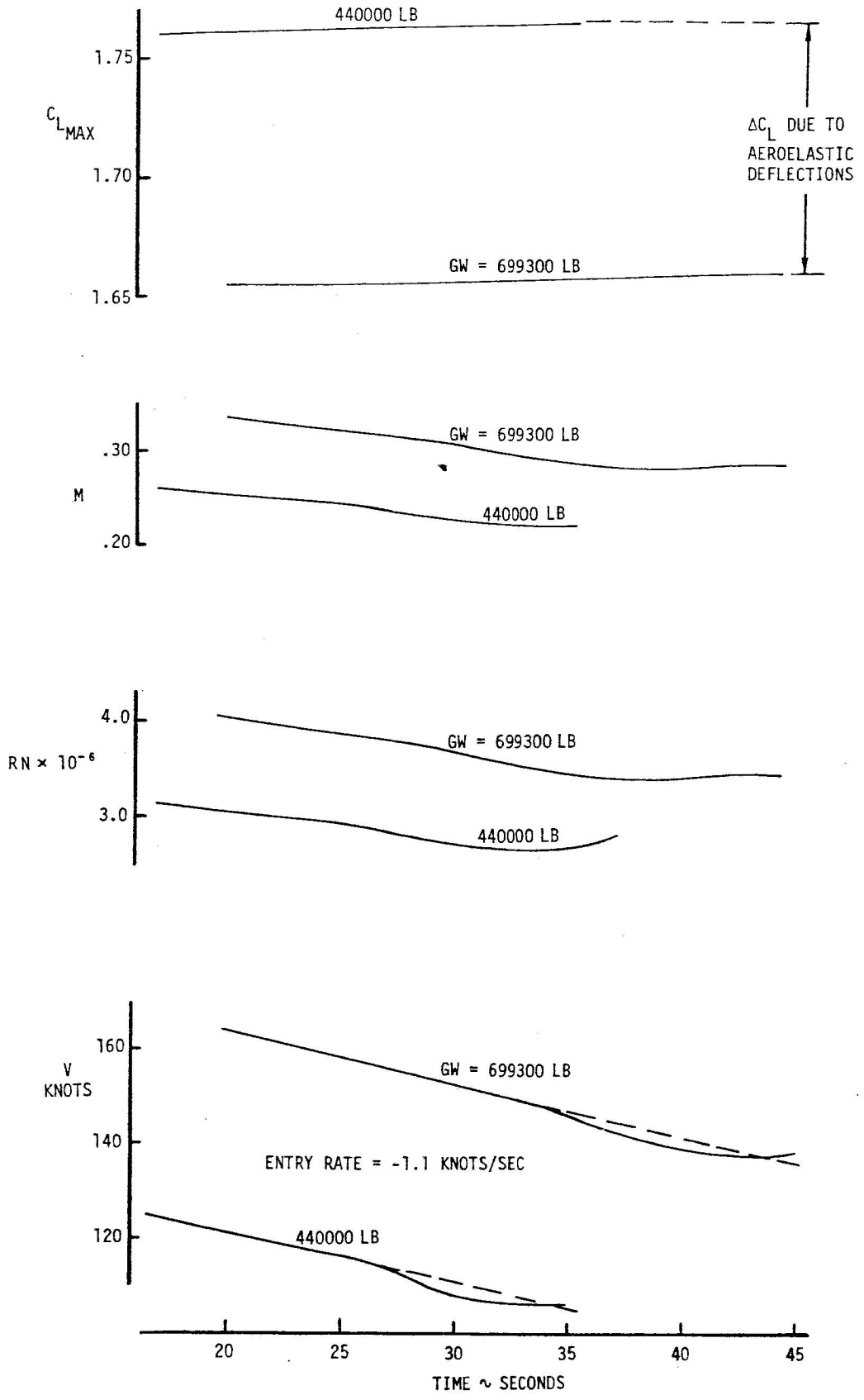

FIGURE 22: VARIATION OF MACH AND REYNOLDS NUMBER DURING TYPICAL STALL AND EFFECT ON $C_{L_{MAX}}$

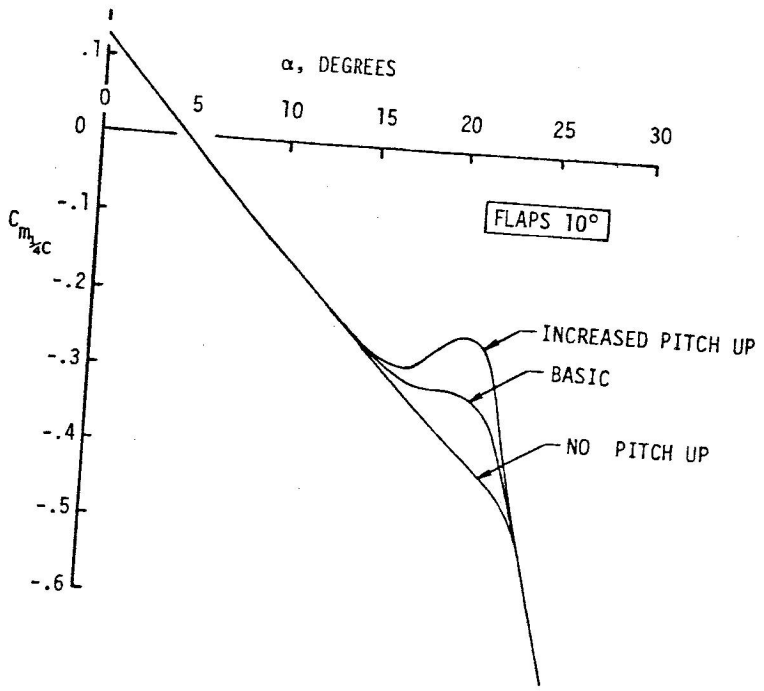

FIGURE 23: PITCHING MOMENTS INVESTIGATED IN STALL SIMULATION

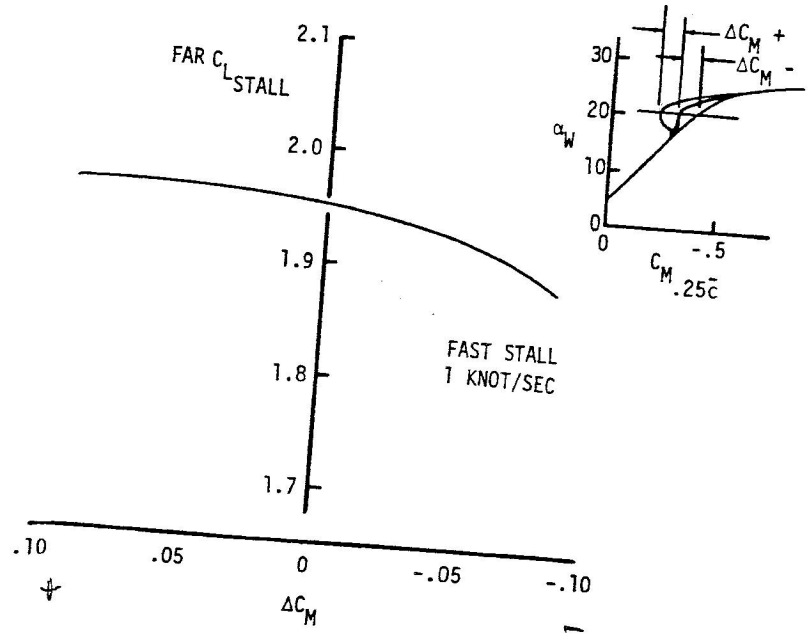

FIGURE 24: EFFECT OF PITCH UP ON STALL LIFT COEFFICIENT

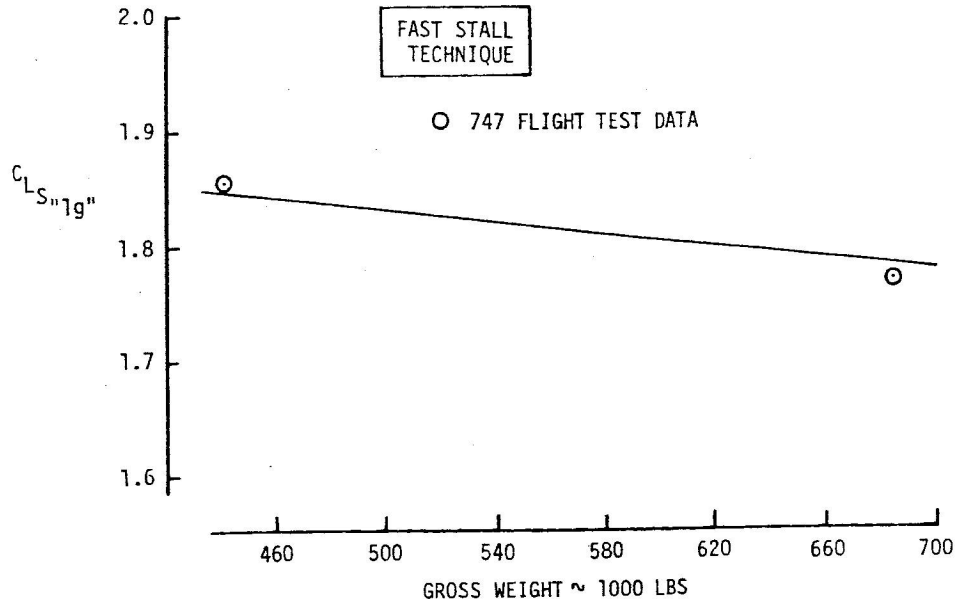

FIGURE 25: EFFECT OF GROSS WEIGHT ON "1g" STALL LIFT COEFFICIENT

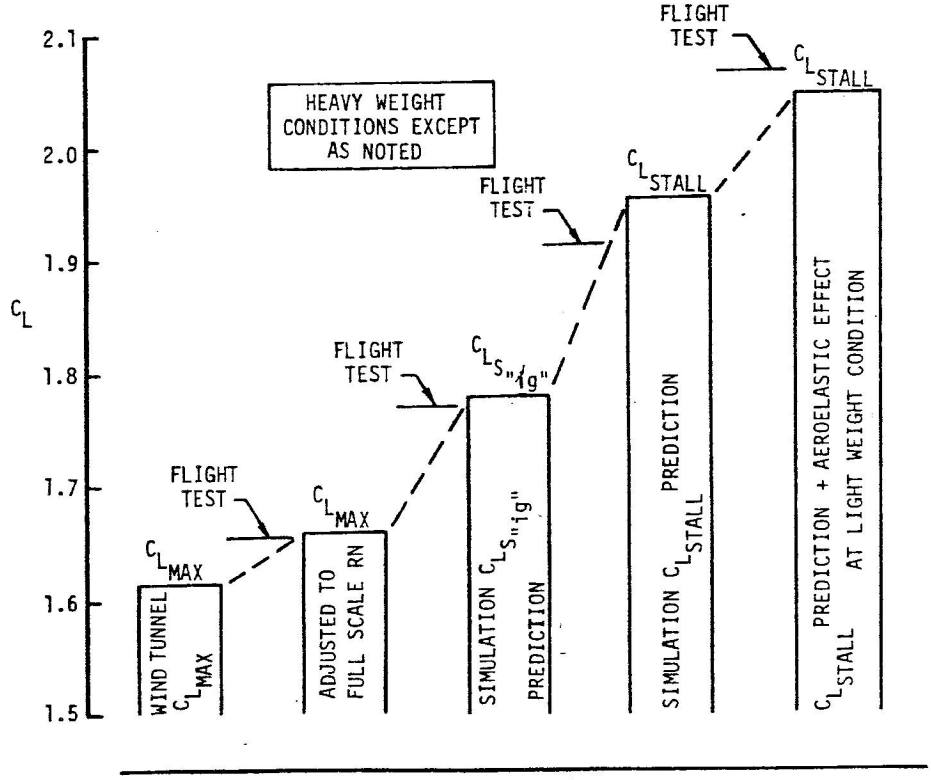

FIGURE 26: SUMMARY BUILDUP OF FAR STALL LIFT COEFFICIENT FROM LOW REYNOLDS NUMBER TUNNEL DATA